Variational Integrators for Constrained Cables

K. Nichols and T. D. Murphey

***Abstract*— Modeling of cable dynamics in cable-suspended robots traditionally focuses on implicit usage of Hamilton's principle or variational calculus to derive a PDE that governs the cable's evolution. An alternative formulation allows one to explicitly use the variational statement to directly calculate the cable's configuration update. Moreover, constraints on cables can experience numerical drift because of the indirect method by which constraints are represented in a PDE setting. Variational methods directly implement the constraint, ensuring that a constraint is satisfied for all time. Variational methods also allow the implicit treatment of constraints through generalized coordinates. In this paper, a special class of integrators known as variational integrators are used to simulate simple cable dynamics, including cables that have multiple constraints, including the catenary as an example.**

I. Introduction

Robotic simulation at times relies heavily on accurate modeling of cable dynamics [15]. Physical plausibility of a resulting solution is key, and indicated by the energy behavior of the system over time. Traditionally, any large divergences between the anticipated solution and the calculated simulation are attributed to the difficultly in representing forces and constraints. The inherent problem in maintaining constraints in ODE and PDE structures is that they set the velocity and other higher derivatives of the body's constraint to zero. The position of the body being constrainted, however, fails to have explicit representation in ODE and PDE structures. We seek a numerical integration technique that explicitly represents and maintains the constraint, resulting in a plausible solution.

Such a technique is developed by using an alternative method that explicitly represents the equations of motion from an energy perspective, generating a Lagrangian function. This is contrary to force balance methods employed by ODE and PDE structures. The integral of the Lagrangian is called the action, which we extremize to form equations of motion. These equations of motion are called the Continuous Euler-Lagrange equations or their discrete counterpart, the Discrete Euler-Lagrange equations, both of which can be numerically integrated to solve for the time evolution of the system.

To construct the Lagrangian and the corresponding action, a generalized coordinate structure is used. In a generalized coordinate structure, constraints between different bodies of the system are implicitly maintained by the coordinate representation. This enables the different segments to stay constrained to each other and not subject to numerical drift.

Given the action we create a numerical update scheme, called a variational integrator. Variational integrators [7], [11], [9] are derived using Hamilton's Principle by minimizing the action integral of the Lagrangian. After utilizing Hamilton's Principle, equations of motion are created and can be integrated numerically. Additionally, these equations can be extended to include forces and constraints. This paper develops such a variational integrator, and demonstrates its use in a variety of simulations. Throughout this paper, we use methods and notation from [14] and [18].

Additionally, this paper employs Finite Element Methods to calculate the potential energy due to elasticity and bending forces. The symbolic integration between variational methods and finite element methods has been explored in several texts [1], [10], [12], [6], [8]. These techniques, however, would be computationally expensive to implement, and not the most practical way to solve dynamics problems.

The paper is organized as follows: Section II discusses a simple example of a one-dimensional pendulum, first deriving the Lagrangian by hand, and then the corresponding continuous and discrete Euler-Lagrange equations. These equations are used in a traditional numerical integration scheme and a variational integrator, respectively. Section III discusses the coordinate representation and structure mentioned earlier needed to represent a multi-dimensional configuration space. Section IV develops a more general method of calculating the Lagrangian for an n-dimensional system. Section V takes the Lagrangian and derives the continuous and discrete Euler-Lagrange equations to be used in an n-dimensional variational integrator. We conclude the section with simulation of a ten segment non-extensible cable. Section VI considers elastic cable dynamics including axial tension. We introduce the FEM approach to modeling axial elongation and bending forces. The variational integrator is then expanded to incorporate constraints. This section is concluded with a simulation of a constrained cable. We then conclude our work and make acknowledgments in Sections VIII and IX, respectively.

II. Modeling of a One Degree of Freedom Pendulum

We first consider a one degree of freedom pendulum swinging with no dissipative forces, as the expected solution is intuitive. In particular the equations of motion generated by calculating the kinetic and potential energies can be derived by hand using energy methods or $\tau = J\alpha$. With this example

This work was supported by two grants from the National Science Foundation, the Colorado Advantage award EMSW21-MCTP #0602284 and CAREER award CMS-0546430

K. Nichols is an undergraduate junior and T. D. Murphey is an Assistant Professor in the Department Electrical and Computer Engineering, University of Colorado at Boulder, Boulder, CO 80309, USA {kirk.nichols,murphey}@colorado.edu

we have an excellent opportunity for comparing variational integrators against other more common numerical integration techniques.

We consider the coordinate representation with θ being the angle of the pendulum from the x-axis and fixed length of the pendulum set to 1. For simplicity in our illustrative example, the mass of the pendulum is additionally set to 1. The Lagrangian, from which the equations of motion are derived, is simply calculated as the kinetic energy of the system minus the potential energy of the system.

$$L(q, \dot{q}) = K(q, \dot{q}) - V(q) \tag{1}$$

The kinetic energy of our one degree of freedom pendulum is $\frac{1}{2}\dot{\theta}^2$. The potential energy or the system involves calculating the z-component of the pendulum and multiplying by gravity. Expressed in θ coordinates: $g(1 - cos(\theta))$. The Lagrangian can now be calculated.

$$L(\theta, \dot{\theta}) = \frac{1}{2}\dot{\theta}^2 - g(1 - cos(\theta)) \tag{2}$$

In solving the one degree of freedom pendulum, we first must utilize the Euler-Lagrange (EL) equations for purposes of generating an ODE which uniquely describes the system.

$$\frac{d}{dt}\frac{\partial L(q, \dot{q})}{\partial \dot{q}} - \frac{\partial L(q, \dot{q})}{\partial q} = 0 \tag{3}$$

For our simple one degree of freedom pendulum, we obtain one ordinary differential equation.

$$\ddot{\theta} + gsin(\theta) = 0 \tag{4}$$

The Euler-Lagrange equation can be solved with the numerical integrator of our choosing, whether it be implicit Euler integration, Runge-Kutta integration, or other methods.

For the purpose of implementing a variational integrator, the Lagrangian must be discretized. The discretized Lagrangian is formulated by modifying the continuous Lagrangian using a backward-difference formulation for $\dot{\theta}$, $\dot{\theta} \rightarrow \frac{\theta_k - \theta_{k-1}}{t_s}$, where t_s denotes the timestep used. . Additionally, we must now utilize the Discrete Euler-Lagrange (DEL) equations, discussed in Section V.

$$D_1 L_d(q_{k-1}, q_k) + D_2 L(q_k, q_{k+1}) = 0 \tag{5}$$

Equation (5) uses the configuration state at times $k - 1$, k, and $k + 1$. D_1, D_2 represent the partial derivatives with respect to the first and second arguments, respectively [18].

For our one degree of freedom configuration space in θ, we generate one Discrete Euler-Lagrange equation.

$$\frac{\frac{\theta_k - \theta_{k-1}}{t_s} - \frac{\theta_k + \theta_{k+1}}{t_s}}{t_s} - g * sin(\theta_k) = 0 \tag{6}$$

Eq. (6) can then be used as a variational integrator after setting θ_0 and θ_1. After initializing with θ_0 and θ_1 in (6), we are able to calculate θ_2 using a root-finding method and we can the reuse (6), plugging in our known values of θ_1 and θ_2 to solve for θ_3 and so on in an iterative fashion. Note that the backward difference acceleration approximation can directly been seen on the left in Eq. (6) and therefore we see the direct correspondence between Eqs. (6) and (2).

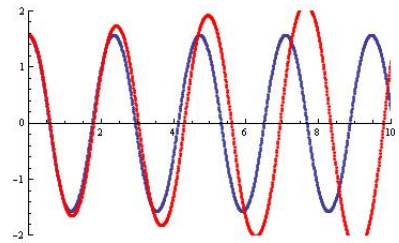

Fig. 1. Euler Integration and Variational Integrators in Modeling a 1 Degree of Freedom Pendulum

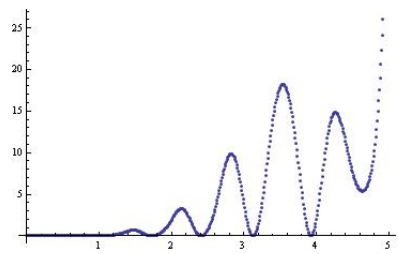

Fig. 2. Error Between Euler Integration and True Solution

Figures 1, 2, and 3 show three different figures relating the effectiveness of the variational integrator modeling the one-link pendulum. The first figure shows high resolution ($t_s = 10^{-2}$) solutions produced by the variational integrator and explicit Euler integration. The solutions are not in agreement, with the explicit Euler integration diverging significantly even before the completion of one period.

This significant divergence is surprising as the time resolution is high and we are only considering a short interval of time. Figure 2 shows the root mean squared error of the Euler method compared to a benchmark numerical solution calculated from Eq.(3) on the interval $t_s \in [0, 10]$. The third figure shows the variational integrator generated solution with $t_s = 0.2$, a low resolution. The solution has not diverged from the expected sinusoid. In fact, t_s can be increased to even greater amounts while still generating a plausible solution. We note, however, that the generated solution at the low resolution is phase shifted from the true solution.

It can be clearly seen that compared to conventional integration methods, variational integrators have a distinct advantage in generating a plausible solution and can even

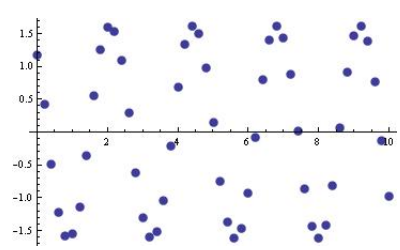

Fig. 3. Low Resolution Simulation Generated by Variational Integrator

compute plausible solutions in a low-resolution setting.

III. Coordinate Representation

Generalized coordinates allows different bodies of a mechanical system to be expressed relative to one another, instead of independently. Therefore, considering a two-link system as an example, the first link would be expressed relative to the origin, while the second link would be expressed relative to the first link. With the links expressed in this manner, the connections between the links are preserved throughout simulation. This is in contrast to using Euler integration on the PDE structure, where due to numerical drift, links of the body separate and produce non-plausible results.

The transformations we consider between two bodies are rigid body transformations. In the XYZ coordinate system, rotations will be expressed as their corresponding Euler angles [14]. A transformation matrix is created to transform one set of coordinates to another to represent one body's position relative to the body before it. We first introduce q, which holds all of the configuration variables of interest.

$$q = \{q_1, q_2, \ldots, q_n\} \tag{7}$$

We additionally introduce a twist, which represents the body velocity. A twist is of the form. $\xi = \{T_X, T_Y, T_Z, R_X, R_Y, R_Z\}^T \in \Re^{6\times 1}$ [14], where T_i and R_i are translations and rotations about the ith axis. For example, a revolute joint rotating about the Y axis with velocity $\dot{\theta}$, as in our one degree of freedom example, has a twist $\xi = \{0, 0, 0, 0, 1, 0\}\dot{\theta}$.

The last tool we need to construct our forward-kinematic representation of the mechanical system is $\hat{\xi}$, as defined in (8) where a_i represents the ith variable of ξ.

$$\hat{\xi} = \begin{bmatrix} 0 & -a_3 & a_2 & a_4 \\ a_3 & 0 & -a_1 & a_5 \\ -a_2 & a_1 & 0 & a_6 \\ 0 & 0 & 0 & 0 \end{bmatrix} \tag{8}$$

In homogeneous coordinates, a transformation matrix $g_{a,b} \in \Re^{4\times 4}$ transforming a body from frame a to frame b contains a rotation matrix of size $R_{a,b} \in \Re^{3\times 3}$ besides a $p_{a,b} \in \Re^{3\times 1}$ translation vector.

$$g_{a,b} = \begin{bmatrix} R_{a,b} & p_{a,b} \\ 0 & 1 \end{bmatrix} \tag{9}$$

We can compound transformation matrices using Eq. (10), which expresses the ith element relative to spatial frame s.

$$g_{s,i} = e^{\hat{\xi} * q_1} \cdot e^{\hat{\xi} * q_2} \cdot \ldots \cdot e^{\hat{\xi} * q_i} \tag{10}$$

The transformation matrix (10) is generated using twist notation from Eq. (8).

IV. Calculating the Lagrangian

A Lagrangian, as previously defined in (1) requires calculations of the kinetic energy and potential energy.

A. Kinetic Energy

In calculating the kinetic energy, we first introduce the Adjoint, $Ad_{g_{a,b}} \in \Re^{6\times 6}$. This matrix is used to transform twists represented in coordinate frame a to an equivalent twist relative to coordinate frame b.

$$Ad_{g_{a,b}} = \begin{bmatrix} R_{a.b} & \hat{p}_{a.b} R_{a,b} \\ 0 & R_{a,b} \end{bmatrix} \tag{11}$$

Where $\hat{p}_{a,b}$ is of the same form as the upper-left 3×3 matrix in (8).

We are now able to take advantage of representing coordinate transforms as twists and introduce the body velocity Jacobian, which will help us map velocities of subsequent elements up to the element of interest as seen in Eq. (12). The columns of the body velocity Jacobian utilize the Adjoint defined in (11).

$$J^b = [Ad_{g_1} \cdot \xi_1 | Ad_{g_2} \cdot \xi_2 | \cdots | Ad_{g_n} \cdot \xi_n] \tag{12}$$

The transformation matrix $g_i(q)$ is calculated using Eq. (13).

$$g_i = e^{\hat{\xi_i}} \cdot e^{\hat{\xi_{i+1}}} \cdot \ldots \cdot e^{\hat{\xi_{n-1}}} \cdot e^{\hat{\xi_n}} \cdot g(0) \tag{13}$$

In Eq. (13), i is the index of the configuration variable of interest and n represents the final configuration variable. The individual columns of the body velocity Jacobian are used to take the ith configuration variable and create a twist that can be used to calculate the kinetic energy of element i while considering the effects of the subsequent configuration variables. The body velocity Jacobian is then used to map $\dot{q}$ to the velocity of the body (14).

$$V^b = J^b \dot{q} \tag{14}$$

Additionally note that (13) is different from (10) as in (10) transformations begin at the spatial frame and end at q_i and (13) begins its transformation at q_i and ends at q_n, the end-effector.

The kinetic energy of the body can now be calculated.

$$KE = \frac{1}{2} \sum_{elements} V_b^T \cdot M \cdot V_b \tag{15}$$

M denotes the body-fixed inertia tensor matrix, a constant diagonal matrix which can be encoded to incorporate elements of varying sizes and shapes.

B. Potential Energy

The potential energy due to gravity is easily calculated by creating a transformation from the spatial frame to the ith element as in (10), multiplying it by the generalized coordinate representation for a point, $p = \{0, 0, 0, 1\}^T$, and extracting the z-coordinate, as represented by the third element in the point vector p. This is in parallel to the one degree of freedom pendulum example. Potential energy due to other sources, such as electric and magnetic fields may also be calculated, and the potential energy due to springs is derived in VI-A.

$\Rightarrow \delta \int_{t0}^{tf} L(q,\dot{q},t)dt = 0$	$\delta \sum_{k=0}^{n-1} L(q_k, q_{k+1}) = 0$
$\Rightarrow \delta \int_{t0}^{tf} (\frac{\partial L(q,\dot{q})}{\partial q}\delta q + \frac{\partial L(q,\dot{q})}{\partial \dot{q}}\delta \dot{q})dt = 0$	$\Rightarrow \sum_{k=0}^{n-1}(D_1 L(q_k, q_{k+1})\delta_{q_k} + D_2 L(q_k, q_{k+1})\delta_{q_{k+1}}) = 0$
$\Rightarrow \int_{t0}^{tf} (\frac{\partial L(q,\dot{q})}{\partial q}\delta q + \frac{\partial L(q,\dot{q})}{\partial \dot{q}}\frac{d}{dt}\delta q)dt = 0$	
$\Rightarrow \int_{t0}^{tf} (\frac{\partial L(q,\dot{q})}{dq} - \frac{d}{dt}\frac{\partial L(q,\dot{q})}{d\dot{q}})\delta q dt = 0$	$\Rightarrow \sum_{k=1}^{n-1}([D_1 L(q_k, q_{k+1}) + D_2 L(q_{k-1}, q_k)]\delta_{q_k}) = 0$
$\Rightarrow \frac{\partial L(q,\dot{q})}{\partial dq} - \frac{d}{dt}\frac{\partial L(q,\dot{q})}{d\dot{q}} = 0$	$\Rightarrow D_1 L_d(q_{k-1}, q_k) + D_2 L(q_k, q_{k+1}) = 0$

TABLE I

DERIVATION OF CONTINUOUS (LEFT) AND DISCRETE (RIGHT) EULER-LAGRANGE EQUATIONS. THE FIRST AND SECOND STEPS USE COMMUTATION OF MIXED PARTIALS. WE THEN INTEGRATE BY PARTS IN THE CONTINUOUS CASE AND RE-INDEX FOR THE DISCRETE CASE, FOR THE SECOND TO LAST STEP. FINALLY, FOR THE INTEGRAL ON THE LEFT AND THE SUM ON THE RIGHT TO BE ZERO THROUGHOUT ALL TIME, THE ARGUMENT MUST EQUIVALENTLY BE ZERO.

V. LEAST ACTION APPROACH TO CONTINUOUS AND DISCRETE MECHANICS

With the continuous Lagrangian properly defined, we are now able to manipulate the Lagrangian to provide us with equations that can update the configuration space. To this end, we utilize the Least Action Principle which extremizes the action integral by taking the total derivative of the action and setting it to zero. Recall the action integral is defined as the integral of the Lagrangian on $[t_0, t_f]$. The resultant equations are called the continuous Euler-Lagrange Eqs. (3), as introduced in the example of the one degree of freedom pendulum in Section II. Table I goes through the derivation of the EL equations on the left hand side, and a parallel derivation of the DEL equations on the right hand side. Note that the derivation of the equations assume that the endpoints are fixed, although they don't necessarily need to be so [18]. Additionally, integration by parts and its discrete counterpart, re-indexing, are used to complete the derivations for the EL and DEL equations respectively. In summary of Table I, we arrive at the Continuous (3) and Discrete (5) Euler-Lagrange Equations.

A. Variational Integrators

Equation (5) can be used as a numerical integrator to solve for the state of the configuration space throughout time using a root-finding algorithm, in exactly the same fashion as Eq. (6) modeled a one degree of freedom pendulum. The only information required are as many initial configuration states as necessary to uniquely define the discretized velocities of the configuration variables. The conventions used in this paper specify only two initial states necessary to initialize the variational integrator as velocities were approximated using a backward-difference rule.

B. Example: Non-Extensible Cable

The structure in our variational integrator is now appropriate to model a non-extensible cable discretized into 10 sections with revolute joints. Figures 4(a), 4(b), and 4(c) show the initial state of the a 10-segment cable and two other configuration states taken at 2 and 4 seconds into the evolution of the system initially at rest. A simulation of this system over time can be found at *http://robotics.colorado.edu/VICM*.

VI. VARIATIONAL INTEGRATORS WITH CONSTRAINTS AND AXIAL STIFFNESS

In other papers on modeling cable dynamics (e.g., [16], [17]), differential equations are used to model the evolution of the cable. Some papers utilize non-Euclidean coordinates [3], mainly in the application of various rotation matrices, but again, only an implicit use of Hamilton's Principle is used. Additionally, the coordinate representation is unique to the problem, and not generalized. Furthermore constraints in these structures are not represented explicitly. We, however, in Section VI-B, derive a method to implement constraints in a generalized coordinate structure.

A. Potential Energy due to Elasticity

Assume we are to discretize a rubber band or wire into segments to form a mass-spring mesh. Hooke's Law is a convenient and intuitive method for modeling axial elongation of a spring. Now consider a steel cantilever beam; Hooke's law fails to incorporate the stiffness of the beam. For this reason we turn to the finite element method to express the potential energy due to elasticity in generalized coordinates [13]. We first consider a stiffness matrix, K, which allows us to map nodal displacement of the element of interest from equilibrium (for this example, a segment of the cable), to potential energy due to elasticity and stiffness (16). E is Young's modulus of elasticity, L, and A denote the length and area of the element of consideration respectively, and I represents various moments of inertia.

$$K = \begin{bmatrix} \frac{A*E}{L} & 0 & 0 & -\frac{A*E}{L} & 0 & 0 \\ 0 & \frac{12*E*I}{L^3} & \frac{6*E*I}{L^2} & 0 & -\frac{12*E*I}{L^3} & \frac{12*E*I}{L^2} \\ 0 & \frac{6*E*I}{L^2} & \frac{4*E*I}{L} & 0 & -\frac{6*E*I}{L^2} & \frac{2*E*I}{L} \\ -\frac{A*E}{L} & 0 & 0 & \frac{A*E}{L} & 0 & 0 \\ 0 & -\frac{12*E*I}{L^3} & -\frac{6*E*I}{L^2} & 0 & \frac{12*E*I}{L^3} & -\frac{6E*I}{L^2} \\ 0 & \frac{6*E*I}{L^2} & \frac{2*E*I}{L} & 0 & -\frac{6*E*I}{L^2} & \frac{4*E*I}{L} \end{bmatrix} \quad (16)$$

$$x = \begin{bmatrix} \Delta x_i(g_i) \\ \Delta y_i(g_i) \\ \Delta \theta_i(g_i) \\ \Delta x_{i+1}(g_{i+1}) \\ \Delta y_{i+1}(g_{i+1}) \\ \Delta \theta_{i+1}(g_{i+1}) \end{bmatrix} \quad (17)$$

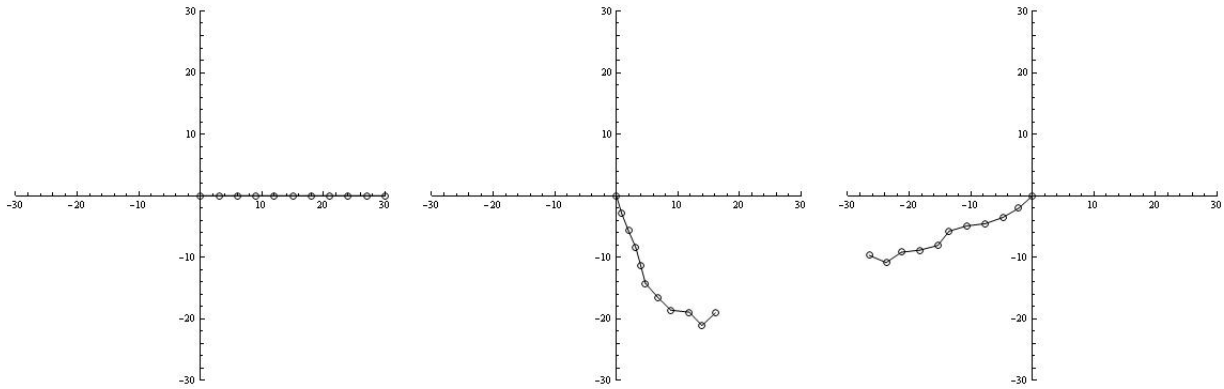

(a) (b) (c)

Fig. 4. (a) Initial Configuration of a 10-link Non-Extensible Cable, (b) 10-link Non-Extensible Cable at 2 Seconds, (c) 10-link Non-Extensible Cable at 4 Seconds. These can be found at *http://robotics.colorado.edu/VICM*.

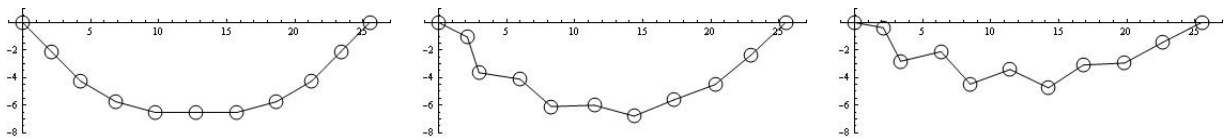

(a) (b) (c)

Fig. 5. (a) Initial Configuration of Cable, (b) Cable Simulation at 1.5 Seconds, (c) Cable Simulation at 3 Seconds. These can be found at *http://robotics.colorado.edu/VICM*.

Notice that nodal displacement representation (17) is different from the representation we used to calculate the kinetic energy of the system. Fortunately, the generalized coordinate structure allows us to map one end of the segment of consideration to the origin. In particular, for each segment of the system specified by $\{\theta_i, L_i\}$, we create a transformation matrix associated with those two elements. This is viable as nodal displacements of one segment of the cable are independent from the nodal displacements of the other segments. After creating our transformation matrix and multiplying it by the generalized coordinate representation for a point, the rigid body is mapped to the origin. Therefore, (17) has only two non-zero elements, $\Delta\theta_i(g_i)$ and $\Delta x_{i+1}(g_{i+1})$. $\Delta\theta_i(g_i)$ directly is θ_i, while $\Delta x_{i+1}(g_{i+1})$ is calculated in (18) assuming $p_{(\theta_i,L_i)} = g_{s,(\theta_i,L_i)}.\{0,0,0,1\}$. Note than in (18), we subtract the equilibrium length of the element, denoted L_{eq} from the actual length of the element as determined by the simulation. With this structure, we can retain our use of generalized coordinates and still be able to express the potential energy due to elasticity. Additionally, this same structure can be extended into 3 dimensions.

$$\Delta x_{i+1}(g_{i+1}) = \|p\|_2 - L_{eq} \tag{18}$$

The potential energy due to elasticity and stiffness is calculated using Eq. (19).

$$V = \frac{1}{2}\sum_{elements} x^T K x; \tag{19}$$

B. Incorporating Constraints

To effectively model constraints associated with a cable, the continuous and discrete Euler-Lagrange equations need to be modified ((20) and (21), respectively). Following the same derivation for creating the Euler-Lagrange and Discrete Euler-Lagrange equations as before, we can account for holonomic constraints. Lagrange multipliers are introduced and used to impart enough force on the system to enforce the constraints.

$$\begin{gathered}\frac{\partial L(q,\dot{q})}{\partial dq} - \frac{d}{dt}\frac{\partial L(q,\dot{q}))}{d\dot{q}} = \lambda\omega(q)^T \\ \frac{d}{dt}(\omega(q)\dot{q}) = 0\end{gathered} \tag{20}$$

$$\begin{gathered}D_2L_d(q_{k-1},q_k) + D_2L(q_k,q_{k+1}) = \langle\lambda, \Delta g(q_k)\rangle \\ g(q_{k+1}) = 0\end{gathered} \tag{21}$$

We note that in Eq. (20), the constraint is "maintained" with $\frac{d}{dt}(\omega(q)\dot{q}) = 0$. Unfortunately, this does not directly represent the constraint, and only represents the velocity of the constraint. Subsequently, due to numerical imprecision in computing and resultant errors, the constraint can undergo numerical drift and the generated solution fails to be plausible. Variational integrators in Eq. (21), on the other hand, represent the constraint with $g(q_{k+1}) = 0$, a direct method which perfectly maintains the constraint as we will see in Figure 6 as discussed in Section VI-C.

C. Results

A elastic cable constrained at both ends modeled using a variational integrator is represented in three different states at time 0, 1.5, and 3 seconds in Figures 5(a), 5(b), and 5(c). A simulation of this cable can be found at *http://robotics.colorado.edu/VICM*. The constraint error calculated from the difference between the simulated constraint from the actual constraint is seen in Figure 6. The constraint

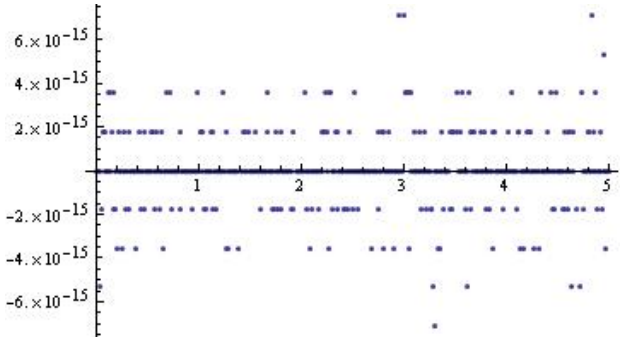

Fig. 6. Error Constructed from the Difference Between the Simulated Constraint and the Actual Constraint

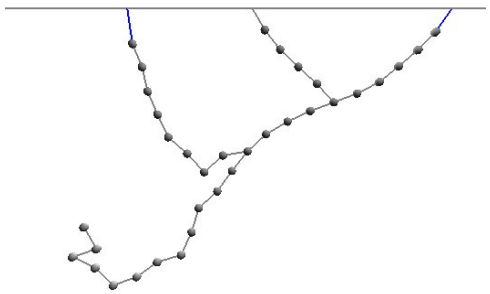

Fig. 7. Entirely Numerical Simulation of Mechanical System

is perfectly maintained, as throughout the entire simulation of 500 data points, the error is on the order of 10^{-15}.

VII. Efficient Implementation

Calculating the Lagrangian as developed above is computationally expensive in the symbolic nature in calculating the Lagrangian. However, new methods for numerically calculating the Lagrangian and all the partial derivatives associated with the Discrete Euler-Lagrange equations have been developed and are quite fast [4], [5]. Figure 7 shows a system with a configuration space modeled with this completely numerical variational integrator, using a software package called `trep` (available at *http://robotics.colorado.edu/trep*. The model has 34 configuration variables, 2 constraints, and with $t_s = 0.02$, takes 79.91 seconds to simulate a 30.0 seconds of motion.

Note that with free-body modeling, there would be 204 degrees of freedom corresponding to each of the elements in the ξ vector. We would additionally have 172 constraints resulting from the two imposed constraints and for ξ vector, 5 of the elements inside the vector must be set to 0, so that only rotations about one axis are permitted.

Other software packages, such as `MAMBO` have been developed to simulate mechanical systems, but fail to use generalized coordinates, resulting in initialization procedures that are tedious [2]. Additionally, `MAMBO` simulates motions desribed by differential equations, which we have shown to be less effective at gerenting plausible solutions.

VIII. Concluding Remarks and Further Developments

Variational Integrators as a numerical integration scheme are an elegant tool in solving both simple and complex dynamic systems with the benefits in *generating plausible solutions with good energy and momentum behavior and perfect maintenance of constraints*. It has been shown here that the Lagrangian can easily be expanded to include other potential energy sources, such as energy resulting from axial elongation and bending. Furthermore, this structure is entirely scalable to larger systems and three dimensions.

The real elegance of variational integrators for cable modeling are presented in their perfect maintenance of holonomic constraints. This emerges in the explicit expression of the constraint in Eq.(21). Additionally, the generalized coordinate structure inherent in the Lagrangian mechanics generates a cable simulation with the different bodies of the system staying connected to each other and the ends of the cable remaining fixed.

There are many more considerations that need to be represented in the variational representation of cable dynamics. Such considerations include slip-stick kinematics, contact dynamics, and constraints that are unilateral, as this paper only utilized continuous constraints.

IX. Acknowledgments

Funding from the National Science Foundation through the Colorado Advantage award EMSW21-MCTP #0602284 supported the research presented here. Additional funding from the National Science Foundation under CAREER award CMS-0546430 also supported this work. Any opinions, findings, and conclusions or recommendations expressed in the material are solely those of the author and do not necessarily reflect the views of the University of Colorado at Boulder or the National Science Foundation.

A special note of thanks goes to Elliot Johnson, who's insight has been truly motivating throughout the course of the research.

References

[1] Abraham I. Beltzer. *Variational and Finite Element Methods: Symbolic Computation Approach*. Springer, 1990.

[2] H. Dankowicz. *Multibody Mechanics and Visualization*. Springer Verlag, 2004.

[3] Vegar Johansen, Svein Ersdal, Asgeir J. Sørensen, and Bernt Leira. Modelling of inextensible cable dynamics with experiments. *International Journal of Non-Linear Mechanics*, 2006.

[4] E. Johnson and T. D. Murphey. Discrete and continuous mechanics for tree representations of mechanical systems. In *IEEE Int. Conf. on Robotics and Automation*, 2008.

[5] E. Johnson and T. D. Murphey. Scalable variational integrators for constrained mechanical systems in generalized coordinates. *IEEE Transactions on Robotics*, Submitted.

[6] Victor N. Kaliakin. *Introduction to Approximate Solution Techniques, Numerical Modeling, and Finite Element Methods (Civil and Environmental Engineering)*. CRC, 2001.

[7] L. Kharevych, U. Tong, E. Kanso, J.E. Marsden, P.Schroder, and M.Desbrun. Geometric, variational integrators for computer animation. In *Eurographics/ACM SIGGRAPH Symposium on Computer Animation*, 2006.

[8] Kyuichiro. *Variational Methods in Elasticity and Plasticity (Monographs in Aeronautics Astronautics)*. Elsevier, 1975.

[9] Adrián Lew. *Variational time integrators in computational solid mechanics*. PhD thesis, California Institute of Technology, 2003.
[10] F.Brezzi M. Fortin. *Mixed and Hybrid Finite Element Methods*. Springer, 1991.
[11] J.E. Marsden and M. West. Discrete mechanics and variational integrators. *Acta Numerica*, 2001.
[12] Piotr Breitkopf Michal Kleiber. *Finite Element Methods in Structural Mechanics: With Pascal Programs*. Ellis Horwood Ltd, 1993.
[13] P. Nthlarasu O.C. Zienkiewixz, R.L. Taylor. *The Finite Element Method*. Butterworth-Heinemann, 2005.
[14] S. Shankar Sastry Richard M. Murray, Zexiang Li. *A Mathematical Introduction to Robotic Manipulation*. CRC, 1994.
[15] Agrawal So-Ryeok Oh, Sunil K. Computationally efficient feasible set points generation and control of a cable robot. *IEEE Transaction on Robotics*, 2006.
[16] U. Storossek. Cable dynamics - a review. *Structural Engineering International*, 1994.
[17] Hiroyuki Sugiyama, Aki M. Mikkda, and Ahmed A. Sahbona. A non-incremental nonlinear finite element solution for cable problems. *Journal of Mechanical Design*, 2003.
[18] Matthew West. *Variational Integrators*. PhD thesis, California Institute of Technology, 2004.